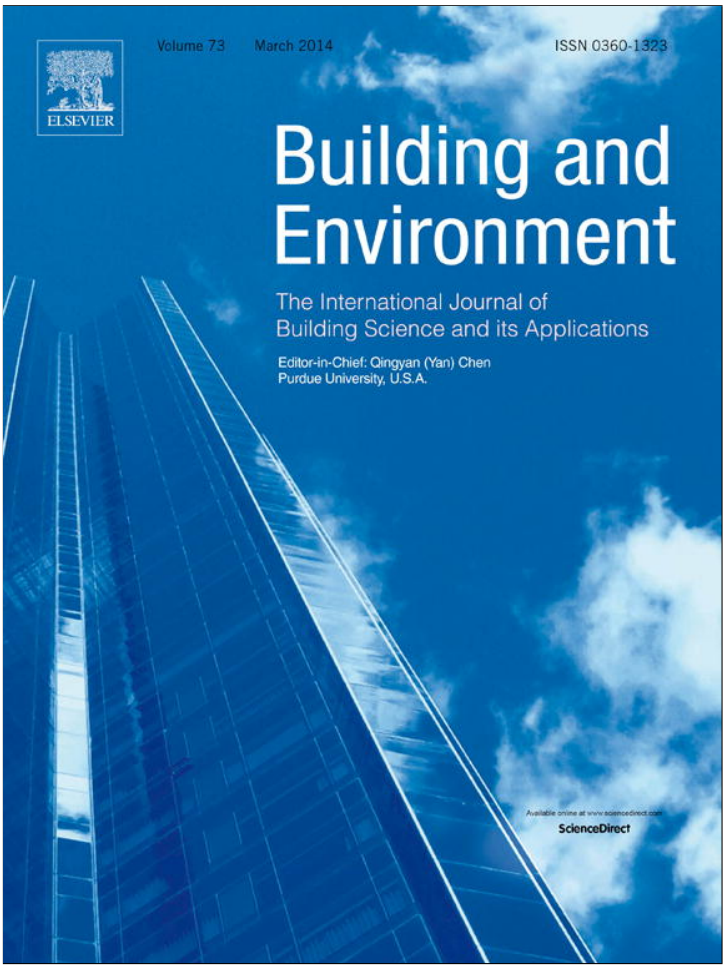

Building and Environment 73 (2014) 75–87

Contents lists available at ScienceDirect

Building and Environment

journal homepage: www.elsevier.com/locate/buildenv

An approach to urban tree daylight permeability simulation using models based on louvers

Ayelén Villalba [a,b,*], Andrea Pattini [a], Erica Correa [a]

[a] INCIHUSA, Instituto Ciencias Humanas, Sociales y Ambientales (Institute of Environmental and Social Sciences) – Laboratorio de Ambiente Humano y Vivienda (Human Environment and Housing Laboratory), CCT – Mendoza, CONICET, CC 131, 5500 Mendoza, Argentina
[b] Pg Postgraduate MAVILE, Faculty of Sciences and Technology, National University of Tucumán, Argentina

ARTICLE INFO

Article history:
Received 30 August 2013
Received in revised form
28 November 2013
Accepted 30 November 2013

Keywords:
Daylight
Urban trees
Raytrace
Solar control systems

ABSTRACT

In oasis cities urban forestation shades the lower level facades of buildings. It is thus crucial to analyze the distributional patterns of sun radiation produced by trees on facades. Nevertheless, the complexity of the canopies requires simplified representations for its study through simulation techniques. On the assumption that lighting behavior of trees, as sun control elements, more closely resembles a louver system rather than other frequently used solar control systems (e.g. perforated obstruction), the present study seeks to verify which of these formal simplifications adjusts better to the real case. The methodology used in this study relies on raytrace simulation of solar control system models generated with hemispherical images. Comparisons are made between measured data of vertical illuminance (lux) in situ and those obtained through simulation for each of the models. Louvers model showed a high degree of adjustment (RMSE 9%). This study may be useful to streamline the analysis of urban trees impact in daylight availability on building facades through simulation.

1. Introduction

Urban forestation can bring solar protection to buildings, reducing energy consumption for interior thermal conditioning due to its shade affect and the phenomena of mass and energy transference that produces the diminishing of temperature in cities. Besides, urban trees reduce erosion, control wind speed and mitigate pollution [1–4].

Added to the benefits related to energy saving, the improvement of environmental conditions and the thermal habitability of space [5,4], there are studies that show the remarkable predilection of people for trees. Getz [6] explains in his works of preference that urban trees have a considerable relevance for people when choosing a residence, and informs that trees contribute significantly in the value of the property due to their aesthetical attributes, comfort associated with attenuation of solar radiation and the increase of privacy [7].

Although, a wide variety of studies examine the impact of urban forestry as a reducer of solar radiation available indoors [8–10], regarding daylighting there are relatively few studies that analyze urban trees as sun control elements for interior spaces. Coder [11], explains the ability of urban forestation for reducing glare; he states that, trees help to control light dispersion and light intensity as well as modifying the predominant wavelengths of their location. He also states that they block and reflect sun light and artificial light, thus diminishing ocular tension, and frame areas lit for architectonic emphasis, security and visibility [11].

These benefits are characteristic in the denominated “oasis cities” -wide streets and intense forestation- for the urban development of arid areas. This is the case of Mendoza city, where the urban forestation is one of the most prominent features of the landscape, wherein the ratio tree-inhabitant is 1:1 [14] (Fig. 1). In the city of Mendoza urban forestry is mainly composed by four species: white mulberry (*Morus alba*), London plane (*Platanus acerifolia*), European ash (*Fraxinius excelsior*) and China berry tree (*Melia azedarach*) [12].

Mendoza city presents semi-arid climate, in this context it is important to use shadow as a strategy to decrease solar radiation, without it, it is impossible to achieve a visually comfortable habitat.

In Mendoza city, the shading strategy is carried out by inserting a vegetable plot that minimizes sun exposure of the metropolitan area [13]. There are detailed studies developed in the city of

* Corresponding author. INCIHUSA – LAHV, Instituto Ciencias Humanas Sociales y Ambientales (Institute of Environmental and Social Sciences) – Laboratorio de Ambiente Humano y Vivienda (Human Environment and Housing Laboratory), CONICET – CCT-Mendoza, CC 131, 5500 Mendoza, Argentina. Tel.: +54 261 45244322; fax: +54 261 5244001.
E-mail addresses: avillalba@mendoza-conicet.gob.ar, ayemv85@hotmail.com (A. Villalba).

0360-1323/$ – see front matter © 2013 Elsevier Ltd. All rights reserved.
http://dx.doi.org/10.1016/j.buildenv.2013.11.026

Fig. 1. Features of study city.

Mendoza which determine the shading affect exerted by urban trees in horizontal surfaces of streets [12].

Regarding the availability of natural lighting in urban areas of the city of Mendoza, Córica [14] claims that: in the oasis city models access to the global availability of visible solar radiation depends on the built environment during winter and on the presence of trees in summer. Availability of solar radiation in summer is directly related to the sky view factor. In the oasis cities, the SVF is very much affected by the presence of afforestation, that is to say, that natural light conditions of urban canyons, in summer, mainly depend on arboreal morphology [14]. It also states that on south sidewalks (north visual) of 20 m wide roads forested with *M. alba* in urban high density areas of Mendoza city (case study of this work), horizontal illuminance is decreased on average 85% throughout the day in summer (maximum leaf development of trees). In summer the availability of vertical illuminance in lower level facades does not reach 10,000 lx in over 70% of the cases [14]. In order to use a solar control or a retro-reflection system on facades, a vertical illuminance of 10,000 lx is required [15]. Thus, it is concluded that, in summer, trees are a "solar control element" for interior spaces illuminated with side windows.

Due to the mentioned effects, urban forestry needs to be analyzed as an environmental item.

Light passing through trees is difficult to simulate [16]. Most lighting and building energy simulation tools assume no exterior obstructions, but it is unlikely to find actual buildings without exterior obstructions, which typically are adjacent buildings and trees. This affects the amount of indoor daylight provided as well as solar heat gain. Therefore, it is very important to take into account all exterior obstructions in lighting and building energy simulation tools [17]. In oasis cities urban forest shades the lower level facades of buildings in summer [14], it is thus crucial to analyze systematically the distributional patterns of visible solar radiation produced by trees on facades. Furthermore the development of predictive simulation models to be used in the study of interior spaces, so as to achieve energy efficiency and visual comfort, is of primary importance.

In particular, for those approaches in which the use of simulation tools is required, the geometrical and optical representation

Table 1
Classification of solar control systems and optical phenomena that they involve.

Textil courtain	Screen panel	Louvers	**Mulberry tree**
Difuse transmitance	Obstruction Direct transmitance	Reflection-redirección	**Obstruction** **Difuse transmitance** **Direct transmitance** **Reflection-redirección**
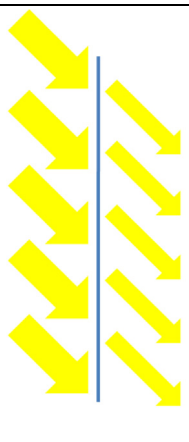	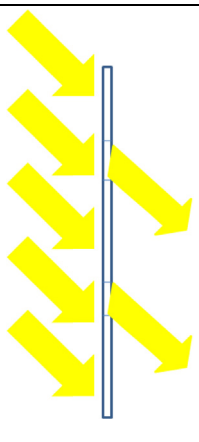	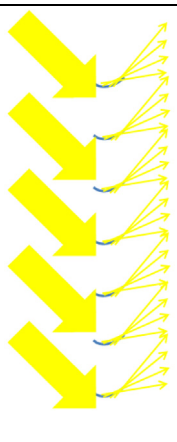	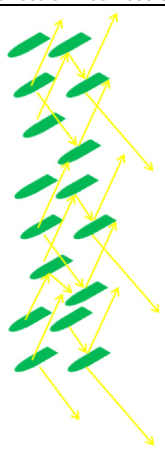

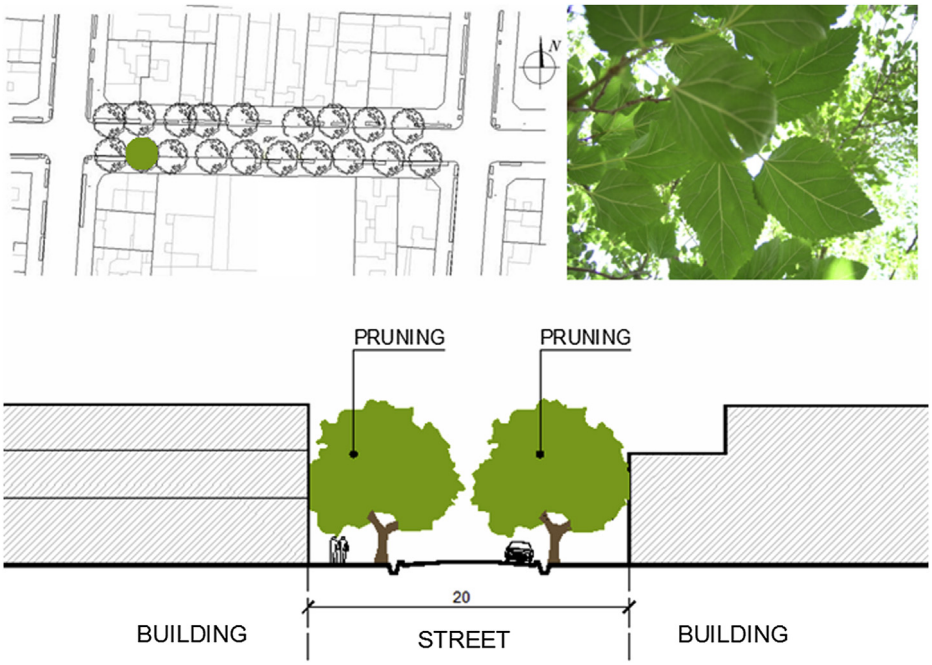

Fig. 2. Morphology of *Morus alba* structure and layout in urban roads of Mendoza city.

becomes highly complex. Thus, it is necessary to know several characteristics of trees such as size, leaf area, leaf reflectance and distribution. Some data such as the magnitude of the grove is easy to find in bibliography, however, there are others such as leaf density and distributional patterns which are difficult to obtain [18]. This situation becomes even more complex for the case of urban trees, whose phenology is modified by the pruning periods, irrigation and urban morphology [19].

Given this context and the complexity of the "canopy" as an element of study, it is necessary to simplify its representation without losing precision. Many simplifications have been made in order to simulate the effect of trees in natural lighting; trees are commonly modeled as transparent surfaces presuming homogeneous visual transmittance [20].

The hypothesis of this study is that, urban trees, in terms of natural light, behave as a solar control system. The three most frequently used phenomena in solar control technics are: diffusion (textile curtain), retroreflection (louvers system with high reflection) and sectorized blocking (screen panel). The present study seeks to verify which of these formal simplifications adjusts better to the real case, by contrasting with vertical illuminance measurements on facades in a forested street.

2. Hemispherical images

The use of hemispherical photography in architectural design is becoming increasingly frequent. Numerous international studies use hemispherical image as a tool in order to determine the influence of buildings and topography in radiation availability in urban spaces. SKY VIEW FACTOR is one of the factors often used to accomplish this characterization [21–26], and the hemispherical photographs assessment is one method to determine this factor.

Lighting studies use hemispherical photography in order to generate luminance maps for glare analysis, among other applications [27,28,18].

Locally there are precedents in the Human Environment and Housing Laboratory, INCIHUSA, related to development of software for hemispherical image analysis. The SKY PIXEL (PIXEL DE CIELO) program has been developed in DELPHI 5.0 and operates in Windows. This tool allows obtaining the sky vision factor value for a certain point through digital JPG format images [29]. This tool has been used in studies of the availability of visible solar radiation, where daily and seasonal solar dynamic, sky vision factors and permeability are shown [14].

Fig. 3. Hemispherical image selected; image converted into black and white pixels; image of vectorized curves extracted from fisheye image.

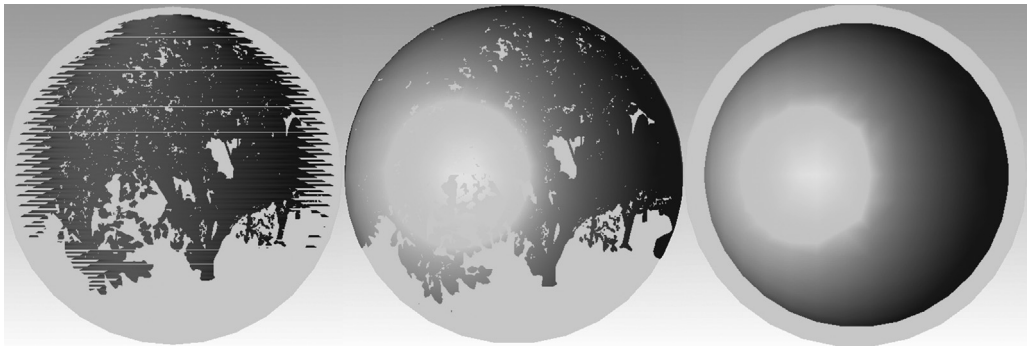

Fig. 4. Projection and subtraction of curves corresponding to the three models: louvers, perforated obstruction and homogenous transmittance (TracePro®).

As regards tree canopies, hemispherical photography and image analysis software constitute fundamental tools [18]. Al-Sallal [30] determines the density of canopies with hemispherical photographs in studies related to the daylighting availability of classrooms. The precision of the 3D model is kept by making the canopy density of the real trees match with the models, based on the image analysis of black pixels (leaves representation) and white pixels (sky representation). In 2009, Al-Sallal [18] develops a method for modeling trees in daylighting simulations using hemispherical images. The method employs high-quality hemispherical photographs which are later analyzed to calculate the visible sky area, used for the theoretical model calculations.

While traditionally tree morphology models per geometrical approximation have a good performance in non-urban fields [31], if we bear in mind the phenological modifications of trees on the urban environment, it is observed that the geometry-based models are quite distant from reality in high density areas.

Thus it is important to employ hemispherical images to describe the tree morphology in urban areas. Therefore, the methodology used in this study relies on simulation models generated with hemispherical images.

3. Methodology

The methodology used in the present study is divided into five stages: acquisition and processing of hemispherical images, virtual model generation (determination of optical and geometrical characteristics), reference measurement, simulation run and statistical analysis of results.

Assuming that tree canopy behaves as a complex fenestration system, it shows different optical phenomena: reflection, diffusion and obstruction, the role of trees as solar light control elements will be modeled according to its similarity to three traditional solar control elements (Table 1):

* homogenous transmittance system (translucent wall), systems which present uniform dimmed transmittance.
  *system of perforated obstruction (screen panel type), this system has a mix of opaque surfaces (transmittance 0) and openings (transmittance 1).
* louvers system, the key phenomenon in this type of system corresponds to light beam redirection.

3.1. Acquisition and processing of hemispherical images

Within the plot of the city of Mendoza, a representative urban enclosure was chosen, facade facing south (north visual), 20 m width road, urban high density, forested with mulberry (Fig. 2). The tree species selected for this study is a *M. alba*, commonly known as mulberry, as it is one of the most widely used species in Mendoza city: 38.27% [32]. Its general characteristics being [12]:

- Average height: 12.5 m (tree typology of second magnitude)
- Average leaf size: length 14.2 cm, width 9.5 cm
- Average trunk perimeter at 1 m height: 1.30 cm
- Trunk diameter: 0.40–0.50 m
- Development Status: good
- Tree canopy width: 10 m average

Based on the selection of a representative sample we proceeded to hemispherical imaging. In this study vertical digital images were taken with a Nikon Coolpix 5400 camera and a Nikon FC-E9 fisheye lens. The advantage of using a Nikon lens is its close to equiangular projection. In previous studies, only a 0.3° value was found to be excluded from the digital image [24]. The images were captured over the frontline of the building at a level corresponding to the middle point of the canopy (Fig. 3). In congruence with the objective of research that seeks to determine, which of the selected models reproduces more accurately access of sunlight to front facades, in presence of street forestation.

Afterward the images were processed with SKY PIXEL software to determine the area of the photo that corresponds to the tree and the area that represents the environment, either street, buildings or sky (Fig. 3). This allows isolating the sectors corresponding to the canopy.

3.2. Virtual model generation (determination of optical and geometrical characteristics)

With respect to the geometrical model, each of the curves corresponding to the empty areas of the tree were determined in a vector graphics editor software (Fig. 3). The virtual models were developed in CAD software; the curves were projected on a laminar hemisphere for the perforated obstruction system and on a hemisphere of multiple elements for the louvers system. In the homogeneous transmittance model the projection is not performed,

Table 2
Direct solar illuminance values.

Hour	Direct illuminance (klux)
10:30	109.17
11:30	112.43
12:30	114.23
13:30	116.45
14:30	114.23
15:30	112.43
16:30	109.17

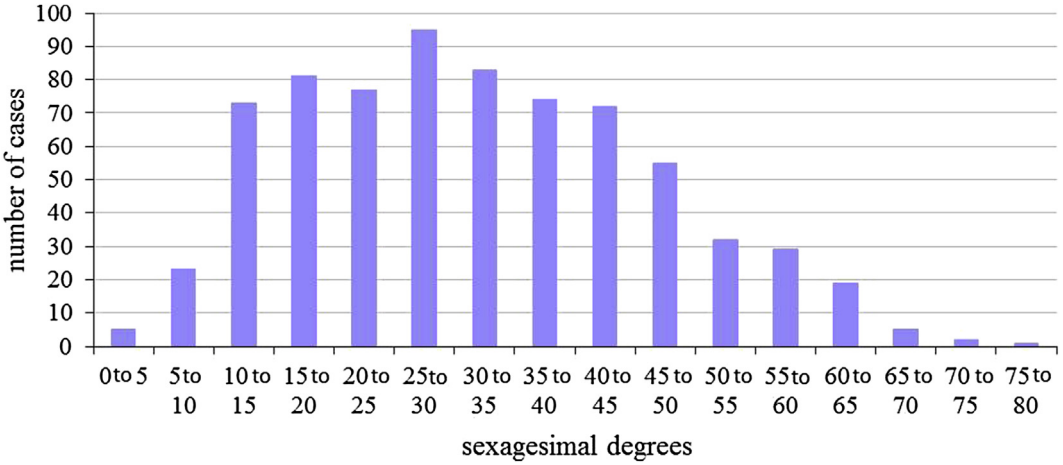

Fig. 5. Histogram: frequency of inclination angle of mulberry leaf in the selected specimens, every 10° degrees.

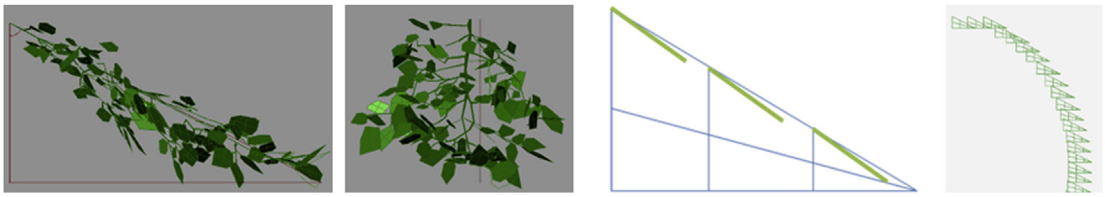

Fig. 6. *Morus alba* branch analysis. 3D models of the inclination angle of branches of the trees studied, distribution and inclination grid of leaves and diagram of branches and leaves disposition.

because the transmittances of the pores are average and distributed isotropically (Fig. 4).

As previously mentioned, information regarding the general dimensional characteristics of the tree was collected for the virtual construction of the three models [19].

Besides the different representations of trees as elements of solar control, other simplified urban elements were added. A vertical surface was used in the back part of the tree model to represent the white wall (flat white paint, 90% diffuse reflecting TracePro®) located in the site of study. A horizontal surface was added to represent the horizontal enclosure of the street.

3.3. Source characterization

Direct normal illuminance, which is measured by orienting the surface so that light impact is normal, was measured for each hour in which the simulation would be carried out in order to determine the characteristics of the incident light source (sun) (Table 2). The obtained data was later employed to characterize the source in the simulated model.

The ray density employed for the simulation was based on the works of Andersen [33], where she determines that for a 6 cm diameter source, 200,000 ray density is sufficient. Proportionally, the amount of necessary rays was calculated for a 100 cm source, the required size for the surface of detection to be completely covered by the incident radiation. A 0.05 flux threshold was employed for ray extinction. It has been verified that a greater number of rays (500,000) or a smaller flux threshold (0.001) do not significantly affect the results, both generated a difference inferior to 1% and significantly prolonged the simulation time [33]. Surface sources were located according to the altitude and azimuth corresponding to the sun position for each of the hours of simulation.

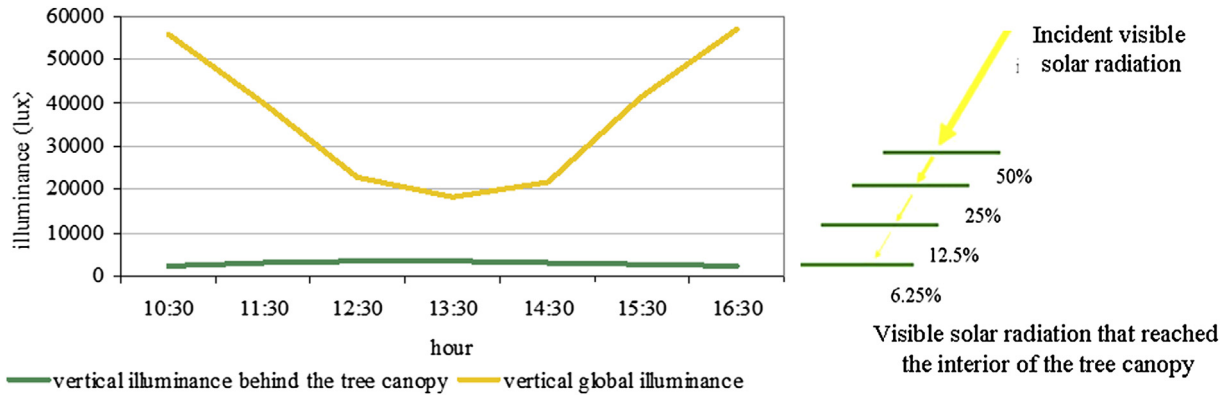

Fig. 7. Attenuation of vertical illuminance. Successive filtrations of radiation caused by leaves (attenuation factor).

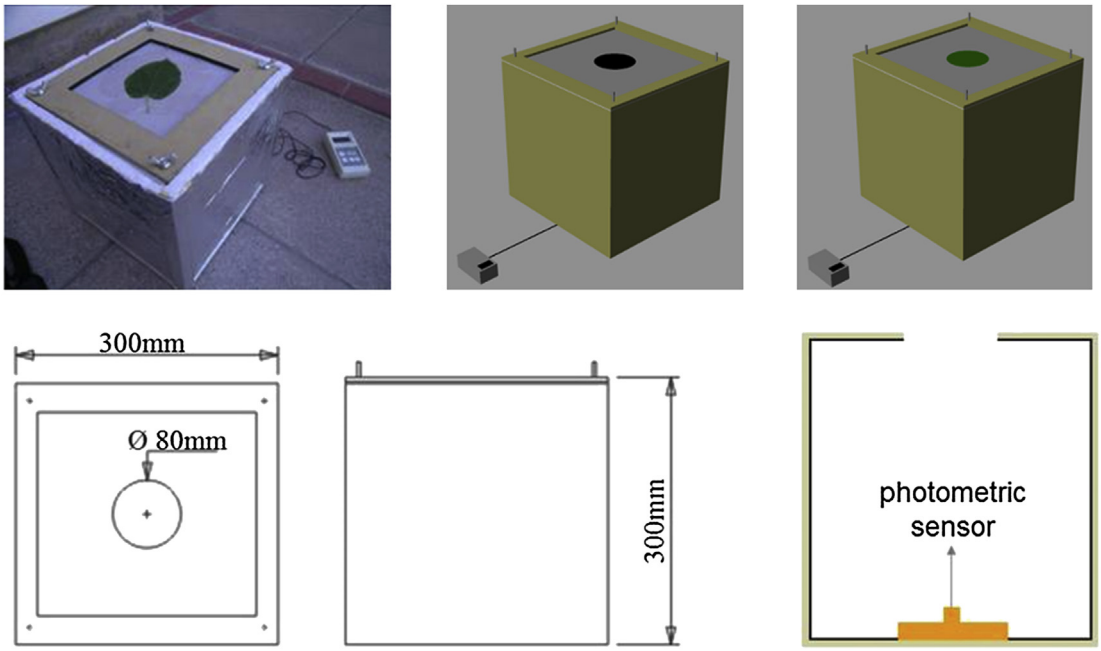

Fig. 8. Measurement diagram of leaf transmittance, without leaf and with leaf. Dimensions of the transmittance measurement box. Photometric sensor location within the transmittance measurement box.

Because the sun behaves as a completely collimated source, a normal angular distribution was selected for the surface source.

Radiation coming from these surface source and incident on the detection surface will be called "global incident radiation" in order to distinguish it from the "reflected incident radiation". The reflected incident radiation also comes from the surface source and is reflected by the horizontal surface (concrete).

3.4. Specific considerations on the louvers model

For the development of the louver model, the predominant angle of inclination of tree leaves was determined, based on the Ryu protocol [34]. The analysis was carried out by taking a sample of 726 leaves corresponding to 20 mulberry specimens located in downtown Mendoza city. The obtained results establish that 60% of the leaves present a 15°–45° inclination, with a mean of 31° 82′ and a median of 30° 33′ (Fig. 5). In order to simplify the model the 30° value was used.

Given previous studies [19] it is known that the average longitudinal size of the mulberry leaf is 14.2 cm, information which turned out to be crucial.

Photos were taken to determine the inclination angle of the peripheral branches. Three-dimensional models were developed with these images in CAD software, where the inclination angle of the branches was measured. An average of 40° degree inclination relative to the horizontal surface was detected (Fig. 6).

This set of geometrical considerations enabled the generation of the virtual model corresponding to the louvers system. A triangular grid was generated according to the inclination angle of leaves and branches which allowed locating the "leaf element" in the outline of the circumference (Fig. 6). These elements were later extruded to form the hemisphere of light shelves.

3.5. Canopy and leaf transmittance

Vertical global illuminance and vertical illuminance under the trees canopy were measured hourly; this data enabled the calculation of canopy transmittance (5%) (Fig. 7). In the perforated obstruction and the homogenous transmittance models, visible solar radiation filtrates only once, thus it is adequate for these models to use the standard transmittance established for canopies.

In the louvers model the distribution elements, following the branch diagram, produce successive filtrations of radiation (attenuation factor) (Fig. 7). This causes reductions in the transmitted light flux, therefore it is correct to use the global transmittance of the material measured according to what Fig. 8 indicates. This implies considering direct solar radiation, strongly directional source, and diffuse light from the sky. The global transmittance measurement was carried out with an LMT photometer POCKETLUX 2A with V lambda filter and cos-correction and an insulated black box, with a perforation at the top where the sample is located, which was routed normally to the sky (Fig. 8), thus registering with and without the leaf element (Fig. 8). The photometric sensor was placed in the bottom of a box (Fig. 8), whose interior is painted with a low reflectance black substrate in order to avoid reflections. Records were taken over several hours to cover variations according to the angle of incidence of the sun. Likewise diffuse transmittance was measured (Table 3). From this analysis it was determined that the average global transmittance of the mulberry leaf is 50%.

Table 3
Diffuse and global transmittance values of *Morus alba*, most common species in Mendoza city.

	White mulberry (*Morus alba*)
Diffuse visible transmittance	0.05
Global visible transmittance	0.53

Table 4
Reflectance in relation to incident angle of radiation of concrete (Ayuntamiento de Barcelona, 2012).

50°	60°	70°	80°
0.151	0.153	0.155	0.157

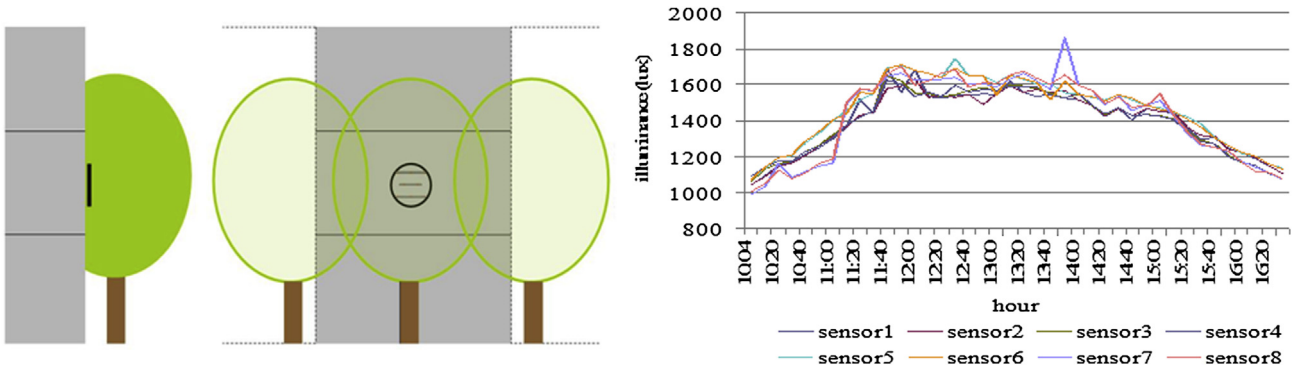

Fig. 9. Illuminance sensors located on the measurement grid. Graphic of vertical illuminance values over facade on forested street, registered by each one of the 8 sensors in a range from 10.00 to 16.30.

Thus considering that the permeability of the mulberry canopy is between 5 and 6% and the transmittance of the mulberry leaf is 50%, in the louvers model, radiation must undergo four stages of filtration (Fig. 7). This analysis enabled optical characterization of the louvers model and determined the arrangement of the light shelves.

Transmittance values are higher than those commonly employed, since the transmittance used in this study is the global rather than the diffuse. Previous studies have shown that light transmittance increases with the incidence of direct light [35]. Therefore diffuse transmittance values obtained for the range of solar spectrum comprehended between 0.38 μm and 0.71 μm agree with other values, such as those established by Oke [21]. This is relevant for this study since the urban environment of the city of Mendoza is exposed mainly to global solar radiation in summer, due to its characteristic sunny weather.

Since, the interaction of leaves with visible solar radiation depends on their physical and chemical characteristics [36], in future studies it would be highly interesting to carry out an assessment of seasonal leaf transmittance. This becomes even more important considering that transmittance of leaves in the visible spectrum is strongly influenced by the concentrations of chlorophyll [37], which varies according to the season.

3.6. Optical considerations common to the three models

The reflectance of leaves was determined according to the Fontoynont [38] measurement protocol, which allows establishing the hemispherical–hemispherical reflectance of lambertian materials. A Minolta LS 110 illuminance meter (1/3° acceptance angle and 0.01–999.900 cd/m^2 accuracy) was used for this measurement, as well as pattern cards. The hemispherical–hemispherical reflectance obtained was 0.11 (11%).

Regarding the horizontal surface, optical properties corresponding to concrete were assigned (Table 4) [39]. Angular reflectance values of concrete were used in some scenarios to adjust the calculated reflected radiation (e.g. scenario A: louvers model, calculated reflected solar radiation) and for others directly inserted as data for the characterization of the material in the simulator (e.g. scenario B: louvers model, simulated reflected solar radiation).

3.7. Scenarios on which simulations were carried out

Different scenarios were assigned according to the characteristics of the models:

A- louvers model, calculated reflected solar radiation.

B- louvers model, simulated reflected solar radiation.

C- perforated obstruction model, simulated reflected solar radiation.

D- perforated obstruction model, calculated reflected solar radiation.

E- homogenous transmittance model, simulated reflected solar radiation.

3.8. Reference measurement

Vertical illuminance measurements (radiometer ILT 1700 multiplexer A415 with an 8 channel selector for multiple detector input SCD110 International Light) over an eight point grid (50 cm diameter) were taken as the reference standard, at first floor facade level (5 m) (Fig. 9). Vertical illuminance values observed at facade level in the context of a forested street oscillate between 1000 lx and 1600 lx (Fig. 9), maximum at solar midday and minimum for the hours when solar altitude is lower. This type of tree reduces global daily vertical illuminance (between 77,000 lx and 23,000 lx) in a significant way (98%) during the day.

In the virtual models the detection surface was placed on the rear vertical surface, according to its position on the facade in the measuring situation (Fig. 9).

The measurement was carried out on December 22nd corresponding to the summer solstice, period in which trees present significant leaf development. Sky condition for the measurement day was corroborated with global and diffuse horizontal illuminance data of the Measurement Station INCIHUSA CCT-CONICET Mendoza (belonging to the International Network of Natural Lighting Measurement Stations IDMP) (Fig. 10).

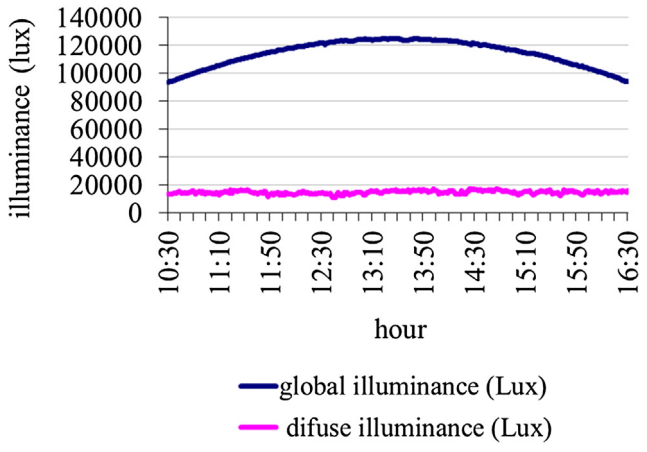

Fig. 10. Data of the sky condition for the day of measurement: global and diffuse hourly illuminance (lux) value.

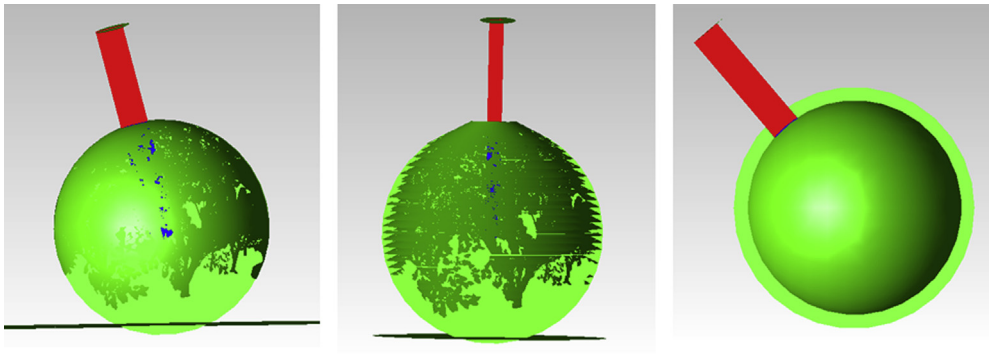

Fig. 11. Ray tracing for the three models: perforated obstruction model, louvers model and homogenous transmittance model (TracePro®).

It was taken into account that, by this time the specimen presents its complete foliar development and, therefore, its maximum expression as solar control element. This condition is important due to the close relation between the availability of natural lighting and the morphological characteristics of the urban enclosure, depending on the season. It should be noted that, only the summer season is examined, because the mulberry is a deciduous species and this determines the absence of foliage in fall and winter season. In spring the species behaves like in summer, due to its brief period of leaf development [19], thus presenting similar conditions, regarding foliage, over a period of approximately 170 days. However it would be extremely useful to repeat the experience in winter, where sun protection provided by deciduous trees is reduced to branches.

3.9. Simulation

The simulations were performed with TracePro® software, a high precision simulator (Fig. 11). TracePro® is a ray tracing program for optical analysis of solid models, which uses a generalized ray tracing method. This technique allows launching rays into a model without making any assumptions as to the order in which objects and surfaces will be intersected. At each intersection, individual rays can be subject to absorption, reflection, refraction, diffraction and scatter. TracePro® uses the ray splitting model of Monte Carlo Simulation [40].

Simulations were performed on a computer with the following general characteristics: CPU: Intel (R) Core (TM) i3-2100 3.10 GHz; RAM 4.00 GB; 64-bit operating system; GPU: ATI Radean HD 5450. Process raytracing data and output is displayed in Table 5.

The simulations were performed every hour from 10.30 to 16.30, which enables to analyze the degree of adjustment of the models to different angles of incidence of solar radiation, in accordance with the solar dynamics.

3.10. Statistical analysis of results

The statistics employed to perform the comparison of the data sets are: root-mean-square error (RMSE) (1) and mean biased error (MBE) (2), their corresponding equations being:

Table 5
Parameters of ray tracing simulation.

50°	60°	70°	80°
0.151	0.153	0.155	0.157

$$\mathrm{RMSE} = \left[\sum_{i}^{n}(E_m - E_s)^2/n\right] \Big/ \left[\sum_{i}^{n} E_m/n\right] \quad (1)$$

$$\mathrm{MBE} = \sum_{i}^{n}(E_m - E_s)/\sum_{i}^{n} E_m/n \quad (2)$$

In which E_m designates the average vertical illuminance values of the 8 points on the grid of measurement for each of the measured hours taken as reference, E_s corresponds to the average vertical illuminance values of the 8 points of the grid of simulation for each hour, n being the number of cases considered.

The RMSE allows determining the difference between the measured and the simulated values.

4. Discussion and result analysis

The louvers model with calculated reflected visible solar radiation presents an RMSE of 0.09, while the louvers model with simulated reflected visible solar radiation shows and RMSE of 0.33 (Table 6). The lowest value of RMSE presented by scenario A in relation to the measured values are due to differences in average lower than 120 lux (Fig. 12). For scenario B the hours corresponding to lower incidence angles (morning and afternoon) present values significantly distant from the measured, an average difference of 500 lx (Fig. 12). This error results from the deficiencies of the louvers model to determine, by simulation, the incident radiation over the facade as a result of the reflection of the concrete. This is because successive reductions of radiation are applied by the

Table 6
Indicates the average vertical illuminance values hourly and the RMSE and MBE for each of the studied scenarios.

	Vertical illuminance (lux)					
Hour	Measure	A	B	C	D	E
10:30	1157	1194	523	938	1654	252
11:30	1504	1440	786	1017	1706	1412
12:30	1621	1812	1639	1987	2829	2199
13:30	1592	1706	1786	1663	2651	2508
14:30	1504	1635	1449	1472	2201	2199
15:30	1311	1463	903	2324	3220	1412
16:30	1099	1249	531	938	1313	252
Average	1398	1500	1088	1477	2225	1462
RMSE		**0.09**	**0.33**	**0.33**	**0.72**	**0.48**
MBE		**−0.07**	**0.17**	**−0.23**	**−0.10**	**0.49**

A- louvers model, calculated reflected solar radiation.
B- louvers model, simulated reflected solar radiation.
C- perforated obstruction model, simulated reflected solar radiation.
D- perforated obstruction model, calculated reflected solar radiation.
E- homogenous transmittance model, simulated reflected solar radiation.

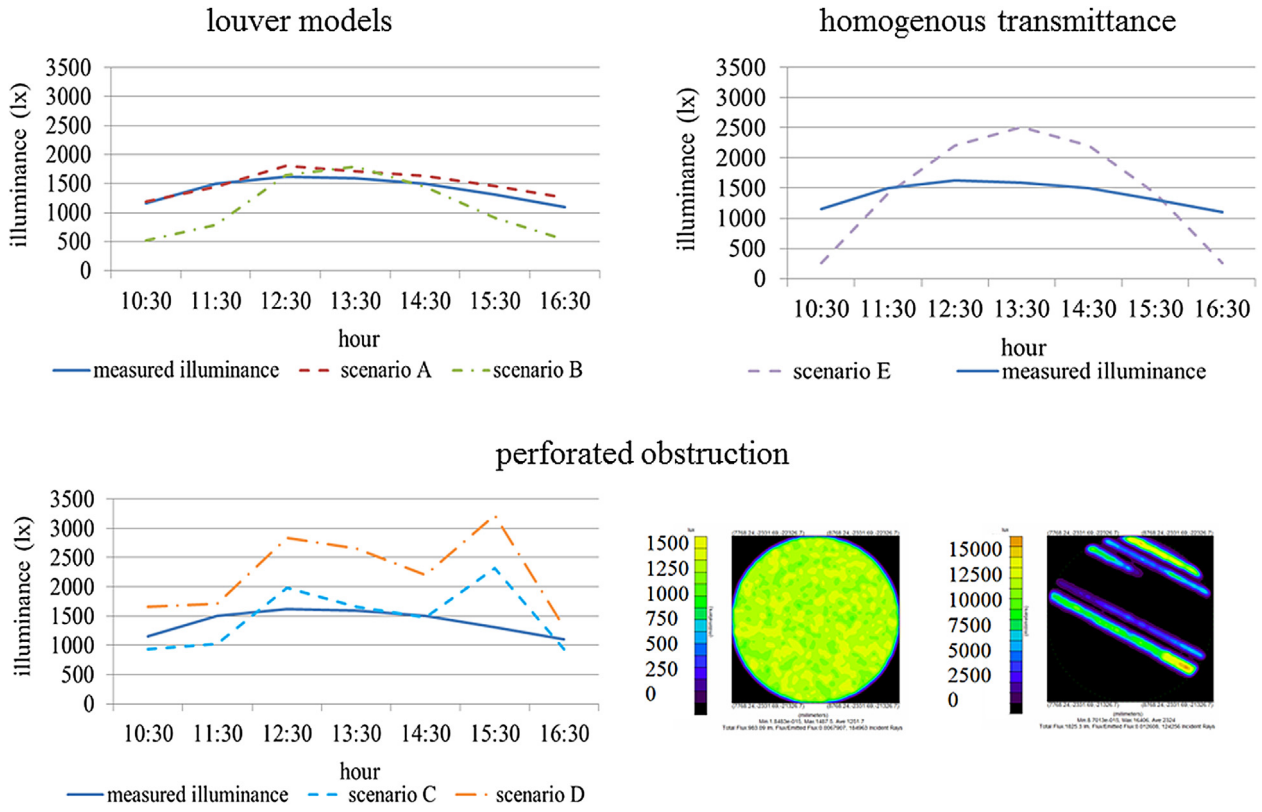

Fig. 12. Hourly illuminance values from 10.30 to 16.30 for the measure reference and models. Distribution of illuminances for the perforated obstruction models when direct vertical solar radiation does not strike and when it does strike (TracePro®).

model. In addition, the data available for the characterization of concrete does not correspond to a complete bidirectional transmittance-reflectance base, which precludes the characterization of the material as a lambertian surface.

For the perforated obstruction models an RMSE of 0.33 was obtained for the scenario of simulated reflected solar radiation (C) and an RMSE of 0.72 for the situation of calculated reflected visible solar radiation (D) (Table 6). These results clearly indicate that this model responds better to simulated reflected solar radiation (scenario C) (Fig. 12), due to its low capacity of attenuation of incident visible solar radiation. However, model C presents difficulties for the calculation of reflected radiation in situations in which its own geometry reduces incident radiation over the horizontal surface (concrete) which later generates reflected solar radiation. Therefore with a detection threshold of 0.05 the reflected radiation is depreciated. If the detection threshold increases (0.005) the reflected radiation can be detected, however, the direct vertical illuminance values increase significantly. Besides, the simulation time is three times longer with respect to the same scenario with a 0.05 detection flux threshold.

The high vertical illuminance values detected represent the most significant misalignments of the perforated obstruction model. This is due to luminous fluxes passing through the perforations (transmittance 1), which generate highly elevated illuminance areas, since it is direct solar radiation. It seems that this is due to the limited ability of this model to reproduce successive reflection and transmittance interactions produced in the real context between the different elements of the canopy. Analysis of vertical illuminance measurement over the facade on a forested street shows that there is no incident direct solar radiation over the detection grid. In Fig. 12 the above situation is displayed.

If we compare these results to the louvers model, we can see that the perforated obstruction scenario with a better response (C) shows a similar root-mean-square error close to the louvers scenario that presents lower adjustment (B).

The model of homogenous transmittance (E) shows a high RMSE value (0.48) (Fig. 12), this situation is due to the lack of treatment from the bidirectional perspective of the system's transmittance. This model rejects the reflected component for all the positions of the source since the incident radiation is filtered by the hemisphere (6% transmittance) in the incoming and outgoing, resulting in radiation available to be reflected by the horizontal surface lower than 5%.

Table 7
Statistical analysis by level.

	Intermediate level sensors		Higher level sensors		Lower level sensors	
	Measured	Simulated	Measured	Simulated	Measured	Simulated
Mean	1369	1431	1407	1434	1409	1452
Standard error	48.78		76.10		71.69	
RMSE	0.04		0.05		0.05	
Correlation coefficient	0.96		0.94		0.95	
R2	0.92		0.88		0.91	

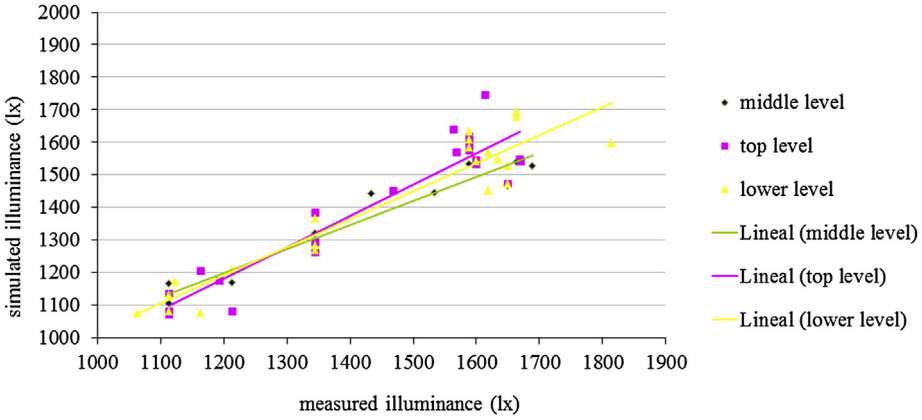

Fig. 13. Correlation between measured and simulated data according to levels.

Table 8
Simulation time: 1 Revision of the entity properties, 2 Preparation of geometry, 3 Ray tracing process. *A and D scenario only simulation time of global solar radiation should be considered.

Model		N° elements	Time (seconds)				
			1	2	3	Subtotal	Total
A*–B	Glo	646	45	15	745	805	1536
	Ref		35	11	685	731	
C–D*	Glo	40	0	10	344	354	1006
	Ref		0	14	638	652	
E	Glo	3	0	0	1397	1397	2860
	Ref		0	0	1463	1463	

Since the louvers model with calculated reflected visible solar radiation presents the closest approximation to the measured data (RMSE of 0.09) a more detailed assay of this scenario performance was conducted. A subsequent correlation analysis between the simulated and measured data (vertical illuminance) was carried out. The analysis was performed by levels according to the arrangement of the sensors on the measurement grid (middle, top and bottom). This study shows that the high correlation detected in the macroscale (average of 8 grid points) remains when performing the analysis by levels. Presenting at the top and bottom elevation RMSE of 0.05, value which is reduced for the middle row to 0.04 (Table 7, Fig. 13).

Concerning the simulation time (with a Intel (R) Core (TM) i3-2100 3.10 GHz processor), the homogenous transmittance model is observed to present the longest simulation time (about 47 min), this appears to be due to the non faceted geometrical disposition. On the other hand, although the perforated obstruction model takes less time of execution, this model adjusts better when both components -global and reflected radiation- are obtained by simulation, while for the louvers model with calculated reflected radiation the time is even shorter since only the global radiation simulation must be effected (Table 8).

In a more detailed way we observe, the numbers of components presented in the models are representatively different; this is displayed in the times of the revision of the entity properties and the preparation of the geometry processes (Table 8).

5. Application example: simplified louver model applied to building simulation

In order to test the performance of the louvers model in ray-tracing simulation softwares for daylighting calculations, DIVA software was used [41]. This software is a sustainable analysis plugin for Rhinoceros 3D Nurbs [42] modeling program applied to perform detailed daylighting calculations in RADIANCE [43]-DAYSIM [44] settings. From this set of simulators illuminance maps and luminance distribution under different climatic conditions (Perez sky model) are obtained [45,46].

To run the software, simulation parameters, climate data and geometric parameters were previously determined. Regarding the first aspect, the radiative rebounds were increased from 2 to 3, taking into account the phenomenon of retroreflection, typical of louvers system. Another simulation parameter considered is the proper depiction of the leaf material within the model. This material was loaded in the file C:\DIVA\Daylight\material.rad, within the data set of glazing materials, since it is a translucent material. Transmittance value is entered into an excel sheet generated to convert transmittance values into transmissivity [47], thereby the complete characterization of the translucent material is achieved. Regarding the climatic base employed, it corresponds to the city of Mendoza [48], where the measurements were registered. The space used for the simulation is an office of 3 m wide, 2.5 m high and 6 m

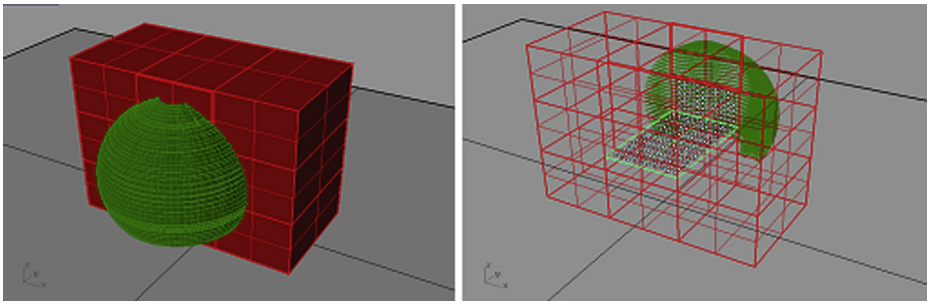

Fig. 14. Front view of the model generated in Rhinoceros 3D Nurbs. Rear view of the model, where node grids can be observed.

Table 9
Simulation results in DIVA. Vertical illuminance measured values (ME). Simulated vertical illuminance values. Simulated horizontal illuminance values.

	vertical illuminance (facade)			horizontal illuminance (work plane)		
hour	M E	Simulation E		Simulation E		
10:30	1157	mean E: 923 A 300-2000: 95 A>2000: 5 A<300: 0	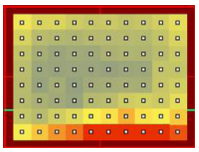	mean E: 697 A 300-2000: 33.3 A>2000: 12 A<300: 54.7	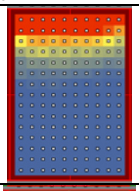	
11:30	1504	mean E: 1158 A 300-2000: 92.5 A>2000: 7.5 A<300: 0	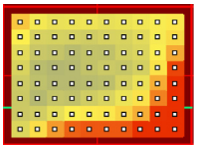	mean E: 845 A 300-2000: 38 A>2000: 12.7 A<300: 49.3	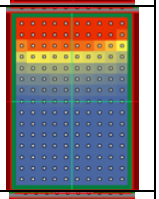	
12:30	1621	mean E: 1555 A 300-2000: 80 A>2000: 20 A<300: 0	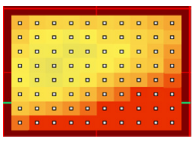	mean E: 1173 A 300-2000: 40.7 A>2000: 18 A<300: 41.3	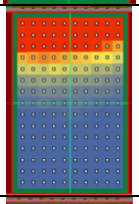	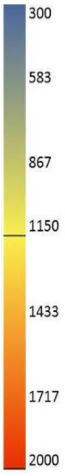
13:30	1592	mean E: 1667 A 300-2000: 78.8 A>2000: 21.2 A<300: 0	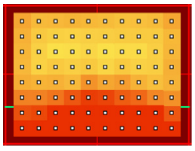	mean E: 1297 A 300-2000: 44 A>2000: 18.7 A<300: 37.3	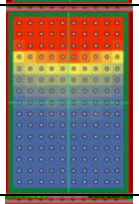	
14:30	1504	mean E: 1539 A 300-2000: 81.2 A>2000: 18.8 A<300: 0	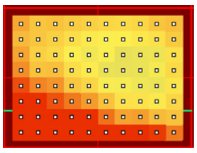	mean E: 1169 A 300-2000: 40 A>2000: 18.7 A<300: 41.3	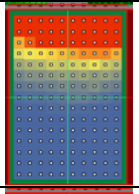	
15:30	1311	mean E: 1150 A 300-2000: 92.5 A>2000: 7.5 A<300: 0	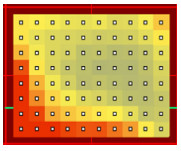	mean E: 836 A 300-2000: 39.3 A>2000: 12.7 A<300: 48	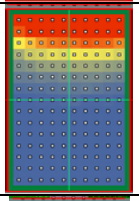	
16:30	1099	mean E: 931 A 300-2000: 93.8 A>2000: 6.2 A<300: 0	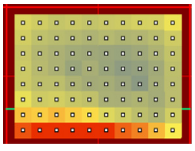	mean E: 703 A 300-2000: 31.3 A>2000: 12 A<300: 56.7	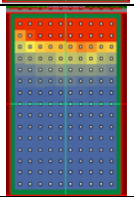	

long. This space was located in a setting of 9 identical office blocks (Fig. 14), data was recorded in the central office of the set, were the tree louver model was placed. Illuminance data was registered over two node grids, one of the grids located on the facade and the other in the interior space at a height of 0.8 m (work plane). Regarding the louvers model, formal simplifications were applied to surface perforations, in order to reduce simulation time.

With this set conditions, simulations were executed hourly (ditto hours that measurement was performed) in order to obtain illuminance maps according to grids. In this type of simulation DIVA gives as outcomes the average illuminance of all grid points in three ranges: the percentage of area presenting illuminance between 300 lx and 2000 lx (visual comfort range), the percentage area having values above 2000 lx and the percentage area that lies below 300 lx (Table 9). From results obtained (Table 9), it was determined that simulated vertical illuminance values on the facade are close to measured data, presenting a 10% error and an R2 of 0.82, which demonstrates a high degree of correlation. Each of the simulations was carried out in an average time of 4 min. Execution speed along with the simplicity of virtual modeling

allows the simulation for different hours and days of the year with a high level of adjustment and without major execution times.

6. Conclusions

The degree of adjustment of the three models based on solar control systems was verified concerning the behavior of the public urban forest with respect to visible solar radiation. The methodology employed is based on hemispherical images and raytracing simulation, validating the simulation results with measurements in situ of vertical illuminance values. Given the high complexity presented by the studied element, the deficiencies of each virtual model in the reproduction of reality were analyzed.

The louvers model with calculated reflection (scenario A) shows a higher degree of adjustment (9% error) with respect to measured data. This is due to the models higher capacity for interaction with radiation, through interreflections and filtering, given its disposition and physical properties. The high level of correlation increases with the detailed analysis performed by levels. The foregoing confirms urban trees in oasis cities behave as a complex fenestration system, where the phenomena of obstruction, direct and diffuse transmittance, reflection and redirection take place. Besides, regarding simulation times, scenario A demands the shortest time, which makes this model even more convenient.

Furthermore, models that base their performance primarily in transmittance phenomena, as homogeneous transmittance and perforated obstruction models, need to be approached from a bidirectional perspective, since they do not have the capacity to interact with incident radiation beyond transmittance. In further studies approaches to bidirectional transmittance for perforated obstruction and homogenous transmittance models will be carried out.

Raytrace simulation with the ray splitting model of Monte Carlo is suitable for this type of analysis because it includes the phenomena of transmission, reflection and absorption, without prior assumptions regarding how radiation intercepts the model. Finally, it has been proved that TracePro is adequate for the accurate representation of the optical and geometric characteristics of complex models such as urban trees.

The use of hemispherical images is an accurate tool for characterization of urban trees in this type of study, as it considers changes in the phenology of trees by pruning, irrigation and urban morphology itself.

Finally, in terms of natural lighting, it has been shown that urban trees act as solar control systems on lower levels facade, and presenting a high degree of similarity to a louver system with a certain level of transmittance. This study does not determine the efficiency of urban trees as a solar control system on facades in the visible spectrum. The need for supplemental protection in the visible range in winter season has been diagnosed in a previous field study, since low angles of incidence (solar altitude) penetrate the interior space, causing glare and visual discomfort [49]. From the solar access perspective, for the urban environment, this deciduous complex fenestration system is beneficial because it is translucent to solar radiation in winter (low solar altitude) and semi-opaque to high summer rays, which generate overheating.

Acknowledgment

The authors wish to thank Dr. Raúl Ajmat for his enlightening advice in simulation assessments.

Authors thank Lambda Research Corporation for concession of the TracePro® Software license used for the studies related to the Doctoral Thesis MAVILE, Faculty of Sciences and Technology, National University of Tucumán, with doctoral CONICET scholarship of the student Ayelén Villalba.

Authors also wish to thank Dr. Lorena Córica, D. I. Juan Manuel Monteoliva and Lic. Juan Pablo Calire.

Nomenclature

E_m	average vertical illuminance for each of the measured hours taken as reference.
E_s	average vertical illuminance for each of the simulated hours.
n	number of cases considered.

References

[1] Mc Pherson E. Functions of buffer plantings in urban environments. Agric Ecosyst Environ 1988;22–23:281–98.
[2] Nowak DJ. Air pollution removal by Chicago's urban forest. In: McPherson E, Nowak DJ, Rowntree RA, editors. Chicago's urban forest ecosystem: results of the Chicago urban forest climate project. Radnor, PA: USDA Forest Service, NEFES; 1994. p. 201. Gen. Tech. Rep. NE 186.
[3] Santamouris M. Energy and climate in the urban built environment. London: James & James; 2001.
[4] Correa EN, Ruiz MA, Cantón A, Lesino G. Thermal comfort in forested urban canyons of low building density. An assessment for the city of Mendoza. Build Environ 2012;58:219–30.
[5] Sudo G, Ochoa JM. Spazi verdi urbani. La vegetazione come strumento di progetto per il comfort ambientale negli spazi abitati. Napoli: Sistemi Editoriali; 2003.
[6] Getz DA, Karow A, Kielbaso JJ. Inner city preferences for trees and urban forestry programs. J Arboric 1982;8:258–63.
[7] Ardone M, Bonnes M. The urban green spaces in the psychological construction of the residential place. In: Bettini V, editor. Elementi di ecología urbana. Torino: Einaudi; 1996.
[8] Brown RD, Gillespie TJ. Microclimate landscape design. New York: Wiley; 1995.
[9] Rosenfeld A, Akbari H, Romm J, Pomerantz M. Cool communities: strategies for heat island mitigation and smog reduction. Energy Build 1998;28:51–62.
[10] Von Stulpnagel A, Herbert M, Sukopp H. The importance of vegetation for the urban climate. In: Sukopp H, Hejny S, Kowarik I, editors. Urban ecology: plants and plant communities in urban environments. The Hague, Netherlands: SPB Academic Pub.; 1990.
[11] Coder KD. Identified benefits of community trees and forests. Athens, GA (US): University of Georgia School of Forest Resources; 1996.
[12] Cantón MA, Cortegoso JL, de Rosa C. Solar permeability of urban trees in cities of western Argentina. Energy Build 1994;20:219–30.
[13] Correa E, De Rosa C, Lesino G. Urban heat island effect on heating and cooling degree days distribution in Mendoza metropolitan area. In: Proceedings of Eurosun 2008. 1th international congress on heating, cooling, and buildings 7th to 10th of October 2008 [Lisbon- Portugal].
[14] Córica L. Comportamiento de la luz natural en entornos urbanos representativos del modelo oasis en regiones áridas. Caso de estudio: ciudad de Mendoza [PhD thesis]. Faculty of Sciences and Technology, National University of Tucumán; 2009. PhD: 299.
[15] Compagnon R. Solar and daylight availability in theurban fabric. Energy Build 2004;36:321–8.
[16] McNeil A. Using annual daylight simulation to evaluate design alternates. In: 8th international radiance workshop 2009.
[17] Yoon Y. Development of a fast and accurate annual daylight approach for complex window systems. College of Engineering, Pennsylvania State University; 2006 [Thesis in Architectural Engineering].
[18] Al-sallal K. Practical method to model trees for daylighting simulation. Using hemispherical photography. In: Proceedings: building simulation. Eleventh international IBPSA conference. Glasgow: Scotland; 2009. pp. 280–5.
[19] Martínez CF. Incidencia del déficit hídrico en forestales de ciudades oasis: caso del Área Metropolitana de Mendoza. Argentina: Biology Postgraduate PROBIOL, Cuyo National University; 2011 [PhD thesis].
[20] Ibarra DI, Reinhart CF. Daylight factor simulations – how close do simulation beginners 'really' get?. In: Eleventh international IBPSA conference Glasgow, Scotland July 27–30, 2009.
[21] Oke TR. Boundary layer climates. 2nd ed. London: Routledge; 1987.
[22] Steyn DG, Hay JD, Watson ID, Johnson GT. The determination of sky-view factors in urban environments using video imagery. J Atmos Ocean Technol 1986;3:759–64.
[23] Chen JM, Black AT, Adams RS. Evaluation of hemispherical photography for determining plan area index and geometry of a forest stand. Agric Forest Meteorol 1991;56:129–43.
[24] Blennow K. Sky view factors from high resolution scanned fish-eye lens photographic negatives. J Atmos Ocean Technol 1995;12:1357–62.
[25] Moin UM, Tsutsumi J. Rapid estimation of sky view factor and its application to human environment. J Human-environ Syst 2004;7:83–7.
[26] Grimmond CSB, Potterb SK, Zuttera HN, Souch C. Rapid methods to estimate sky-view factors applied to urban areas. Int J Climatol 2001;21:903–13.

[27] Kumaragurubaran V, Inanici M. Hdrscope: high dynamic range image processing toolkit for lighting simulations and analysis. In: International building performance simulation association (IBPSA) 2013 conference, Chambery, France 2013. pp. 3400–7.
[28] Ward G. High dynamic range imaging. In: Proceedings of the ninth color imaging conference November 2001.
[29] Correa EN, Pattini AE, Córica L, Fornés M, Lesino G. Evaluación del factor de visión de cielo a partir del procesamiento digital de imágenes hemisféricas. Influencia de la configuración del cañón urbano en la disponibilidad del recurso solar. Avances en energías renovables y medio ambiente 2005;9:43–8.
[30] Al-sallal K, Ahmed L. Improving natural light in classroom spaces with local trees: simulation analysis under the desert conditions of the uae. In: Proceedings: building simulation, ninth international IBPSA conference, Beijing, China 2007. pp. 1168–74.
[31] Campbell GS, Norman JM. The description and measurement of plant canopy structure. In: Russell G, Marshall B, Jarvis PG, editors. Plant canopies: their growth, form and function. Cambridge University Press; 1989. pp. 1–19.
[32] Cantón MA, Mesa A, Cortegoso JL, de Rosa C. Assessing the solar resource in forested urban environments: results from the use of a photographic computational method. Arch Sci Rev 2003;46:115–23.
[33] Andersen M. Innovative bidirectional video-goniophotometer for advanced fenestration systems. Switzerland: Swiss Federal Institute of Technology, Solar Energy and Building Physics Laboratory; 2004 [PhD thesis].
[34] Ryu Y, Sonnentag O, Nilson T, Vargas R, Kobayashi H, Wenk R, et al. How to quantify tree leaf área index in an open savannas ecosystem: a multi-instrument and multi-model approach. Agric Forest Meteorol 2010;150:63–76.
[35] Bousquet L, Lavergne T, Deroin T, Widlowski JL, Moya I, Jacquemoud S. Multispectral and multiangular measurement and modeling of leaf reflectance and transmittance. Photochem Photobiol 2010:96–101.
[36] Jacquemoud S, Baret F. PROSPECT: a model of leaf optical properties spectra remote sensing and environment 1990;34:75–9.
[37] Jacquemoud S, Ustin S. Modeling leaf optical properties. http://www.photobiology.info/Jacq_Ustin.html.
[38] Fontoynont M. Daylight performance of buildings. Lyon: ENTPE; 1999.
[39] Reflectancias suelos urbanos. Ayto. de Barcelona. www.terra.es/personal6/a.fontm/reflec.htm.
[40] TracePro® user's manual. Littleton, MA: Lambda Research Corporation; 2010.
[41] Jakubiec JA, Reinhart CF. The 'adaptive zone' – a concept for assessing glare throughout daylit spaces. Light Res Technol 2011;44:149–70.
[42] Mcneel R, Associates. Rhinoceros Version 4.0; 2010. Service Release.
[43] Ward G, Shakespeare RA. Rendering with radiance. Morgan Kaufmann Publishers; 1998.
[44] Reinhart CF. Lightswitch 2002: a model for manual and automated control of electric lighting and blinds. Solar Energy 2004;77(1):15–28.
[45] Perez R, Ineichen P, Seals R, Michalsky J, Stewart R. Modeling daylight availability and irradiance components from direct and global irradiance. Solar Energy 1990;44(5):271–89.
[46] Perez R, Seals R, Michalsky J. All-weather model for sky luminance distribution – preliminary configuration and validation. Solar Energy 1993;50(3):235–45.
[47] DIVA, excel transmissivity converter. http://diva4rhino.com/user-guide/rhino/custom-radiance-materials.
[48] Monteoliva JM, Villalba A, Pattini A. Impacto de la utilización de bases climáticas regionales en la simulación de alta precisión de iluminación natural. Avances en Energías Renovables y Medio Ambiente 2012;16(1):57–64.
[49] Köster H. Dynamic daylighting architecture: basics, systems, projects. Basel: Birkhäuser; 2004.